Inorganic Chemistry

Article

pubs.acs.org/IC

Influence of the N−N Coligand: C−C Coupling Instead of Formation of Imidazol-2-yl Complexes at {Mo(η^3-allyl)$(CO)_2$} Fragments. Theoretical and Experimental Studies

Andrea Cebollada,[†] Maialen Espinal Viguri,[‡] Julio Pérez,[‡,§] Jesús Díaz,*[,∥] Ramón López,*[,⊥] and Lucía Riera*[,§]

[†]Departamento de Química Inorgánica-ISQCH, Universidad de Zaragoza-CSIC, Pedro Cerbuna, 12, 50009 Zaragoza, Spain

[‡]Departamento de Química Orgánica e Inorgánica, Universidad de Oviedo, Julián Clavería, 8, 33006 Oviedo, Spain

[§]Centro de Investigación en Nanomateriales y Nanotecnología (CINN), CSIC-Universidad de Oviedo-Principado de Asturias, Avenida de la Vega 4-6, 33940 El Entrego, Spain

[∥]Departamento de Química Orgánica e Inorgánica, Universidad de Extremadura, Avda de la Universidad s/n, 10071 Cáceres, Spain

[⊥]Departamento de Química Física y Analítica, Universidad de Oviedo, Julián Clavería, 8, 33006 Oviedo, Spain

Supporting Information

ABSTRACT: New *N*-methylimidazole (N-MeIm) complexes of the {Mo(η^3-allyl)$(CO)_2$(N−N)} fragment have been prepared, in which the N,N-bidentate chelate ligand is a 2-pyridylimine. The addition of a strong base to the new compounds deprotonates the central CH group of the imidazole ligand and subsequently forms the C−C coupling product that results from the nucleophilic attack to the imine C atom. This reactivity contrasts with that previously found for the analogous 2,2′-bipyridine compounds [Mo(η^3-allyl)$(CO)_2$(bipy)(N-RIm)]OTf [N-RIm = N-MeIm, *N*-mesitylimidazole (N-MesIm, Mes= 2,4,6-trimethylphenyl); OTf = trifluoromethanesulfonate) which afforded imidazol-2-yl complexes upon deprotonation. Density Functional Theory (DFT) computations uncover that the reactivity of the imine C atom along with its ability to delocalize electron density are responsible for the new reactivity pattern found for the kind of molybdenum complexes reported herein.

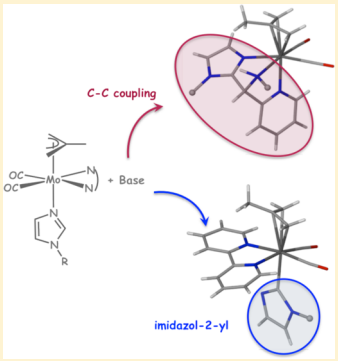

INTRODUCTION

The imidazole moiety is very often encountered in biological systems. The importance of this function is mainly due to its presence in the side chain of the amino acid histidine, and its role as a metal binding site in metalloenzymes.[1] The relatively small size and the electronic properties (σ-donor and π-aceptor) make imidazole and its derivatives good ligands for a variety of metal fragments.[2] Whereas the coordination chemistry of imidazoles has been therefore extensively studied, little attention has been paid to the analogy between cationic metal complexes with *N*-alkylimidazole (N-RIm) ligands and *N*,*N*′-dialkylimidazolium salts instead.[3] In fact, the former can be regarded as N-metalated analogous of the latter (Figure 1).

The deprotonation of an *N*,*N*′-dialkylimidazolium salt affords a N-heterocyclic carbene (NHC).[4] Therefore, we focused our attention in the deprotonation of transition metal complexes with *N*-alkylimidazole ligands, trying to generate, in a similar way, a new type of NHC species with a metal fragment as substituent of one of the imidazole nitrogen atoms.[5] In this research area we have found that the deprotonation of the central C−H group of a coordinated *N*-alkylimidazole affords very reactive species with reaction outcomes strongly depending on the nature of the imidazole substituent and the ancillary ligands.[6] In particular, for Mo(II) cationic compounds of formula [Mo(η^3-C_4H_7)(bipy)$(CO)_2$(N-RIm)]OTf (R = Me, Mes) the addition of a strong base led to imidazol-2-yl complexes resulting from the tautomerization of the heterocycle from N- to C-coordinated once the deprotonation had occurred. The subsequent addition of electrophilic reagents (HOTf, MeOTf, or EtOTf) afforded molybdenum NHC compounds (Scheme 1) by protonation or alkylation of the nonsubstituted nitrogen.[7]

In agreement with the experimental results found for the deprotonation of [Mo(η^3-C_4H_7)(bipy)$(CO)_2$(N-RIm]OTf compounds, a DFT study showed that the most favorable reaction mechanism was reminiscent of the one found for [Mn(bipy)$(CO)_3$(N-RIm)]OTf compounds,[5b,7] involving an

Figure 1. Analogy between imidazolium salts (a) and cationic metal complexes with *N*-alkylimidazole ligands (b).

Received: November 12, 2014
Published: February 27, 2015

DOI: 10.1021/ic502729z
Inorg. Chem. 2015, 54, 2580−2590

Scheme 1. Synthesis of Imidazol-2-yl and NHC Complexes from *N*-Alkylimidazole Derivatives

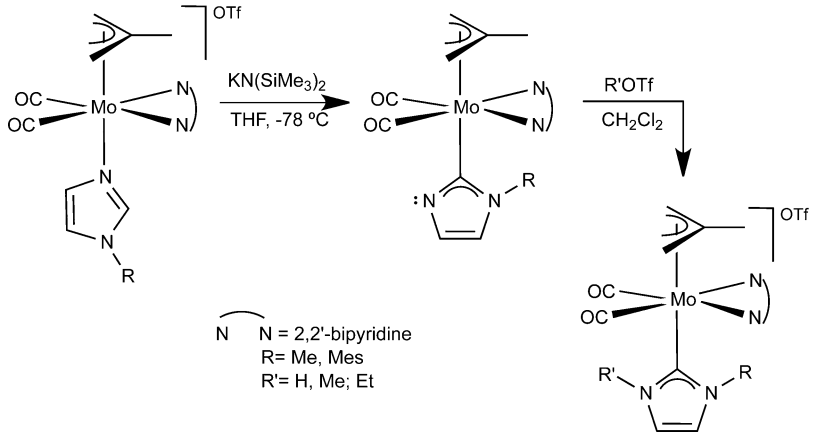

initial attack of the imidazole deprotonated carbon atom onto a *cis*-CO ligand, to afford in a second step imidazol-2-yl species. Furthermore, these calculations pointed out that the difference in energy between this pathway and the one that would lead to C−C coupling products (analogous to the reactivity pattern found for $[Re(bipy)(CO)_3(N\text{-}RIm)]^+$ complexes) is only 3.5 kcal/mol.[7] This result prompted us to investigate the feasibility of inverting the reactivity pattern in $\{Mo(\eta^3\text{-}C_4H_7)(CO)_2\}$ complexes, to obtain C−C coupling products.

Herein we report the synthesis and reactivity of $[Mo(\eta^3\text{-}C_4H_7)(CO)_2(N\text{-}MeIm)(py\text{-}2\text{-}CH{=}N\text{-}R)]OTf$ (R= C_6H_5, C_6H_4-4-Me, C_6H_3-3,5-Me_2, *i*Pr, *t*Bu) compounds, showing that C−C coupling products are obtained upon deprotonation. The DFT computations are in agreement with the experimental findings, and show that the replacement of the α-diimine bipy by the iminopyridines employed in this work results in that the pathway leading to the C−C coupling products becomes preferred.

RESULTS AND DISCUSSION

The labile complex $[MoCl(\eta^3\text{-}C_4H_7)(CO)_2(NCMe)_2]$ reacts with the equimolar amounts of 2-pyridylcarboxaldehyde and aniline in THF to afford complex **1a** as shown in Scheme 2. Its

Scheme 2. One-Pot Synthesis of 2-Pyridylimino Chlorocomplexes 1a−e

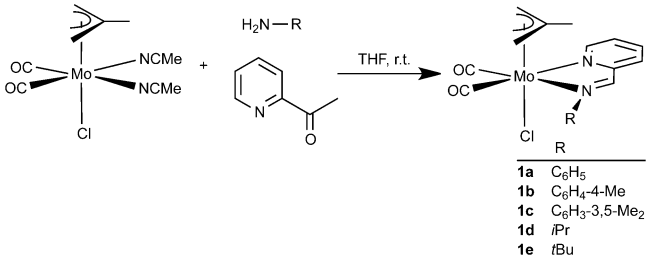

spectroscopic data in solution, and the full characterization of some of its reaction products, discussed below, show that **1a** possesses an iminopyridyl ligand coordinated as bidentate chelate to the $\{MoCl(\eta^3\text{-}C_4H_7)(CO)_2\}$ fragment.

The metal-free reaction of the aldehyde and aniline takes 12 h in refluxing toluene to reach completion.[8] In contrast, the three-component reaction described above produces **1a** in less than 1 h at room temperature, indicating that the metal exerts a significant templating effect, as previously noted by others.[9] It has been proposed that the κ^2-(*N*,*O*) coordination of the aldehyde activates the carbonyl group toward the condensation (enhancing its electrophilic character) making the reaction more favorable.[10]

The employment of 4-methylaniline and 3,5-dimethylaniline afforded, in the same way, complexes **1b** and **1c**, respectively. In contrast, *ortho*-substituted anilines (such as 2,4,6-trimethylaniline or 2,6-diisopropylaniline) precluded the formation of the desired molybdenum iminopyridine derivatives, probably due to the steric hindrance. The new compounds **1a−c** were obtained in good yields, as the only products of the reactions, and their spectroscopic data in solution were in agreement with the proposed stoichiometry and geometry showed in Scheme 2,[11] and similar to related pyridylimino compounds of the fragment $\{MoCl(\eta^3\text{-allyl})(CO)_2\}$.[9d]

The addition of a few drops of acetonitrile to a 1:1 mixture of AgOTf and $[MoCl(\eta^3\text{-}C_4H_7)(CO)_2(py\text{-}2\text{-}CH{=}N{-}Ar)]$ (Ar = C_6H_5 **1a**, C_6H_4-4-Me **1b**, C_6H_3-3,5-Me_2 **1c**) in dichloromethane led immediately to the precipitation of a white solid (AgCl), and the formation of the nitrile compounds $[Mo(\eta^3\text{-}C_4H_7)(CO)_2(NCMe)(py\text{-}2\text{-}CH{=}N{-}Ar)]OTf$. From these species the labile MeCN ligand is easily substituted by addition of the equimolar amount of *N*-methylimidazole (N-MeIm) affording imidazole compounds $[Mo(\eta^3\text{-}C_4H_7)(CO)_2(N\text{-}MeIm)(py\text{-}2\text{-}CH{=}N{-}Ar)]OTf$ (**2a−c**, see Scheme 3).

Scheme 3. Synthesis of Cationic Imidazole 2-Pyridylimino Complexes 2a−e

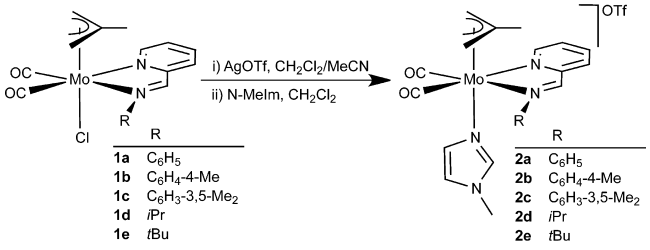

These reactions were followed by IR spectroscopy, showing first the formation of cationic nitrile species (the IR ν_{CO} bands showed the typical pattern for *cis*-$\{Mo^{II}(CO)_2\}$ fragments, and the values changed, from 1951, 1876 cm^{-1} in the case of **1a**, to 1964, 1885 cm^{-1}), and afterward the substitution of the nitrile by the more σ-donor N-MeIm ligand (IR ν_{CO} values downshifted to 1949, 1869 cm^{-1} for **2a**).

DOI: 10.1021/ic502729z
Inorg. Chem. 2015, 54, 2580−2590

^{1}H and ^{13}C NMR spectra in solution of compounds **2a**–**c** showed the asymmetry of the new molecules (as the iminopyridine ligands are nonsymmetric) and the incorporation of one N-MeIm ligand per metallic fragment. The solid state structure of **2c**, determined by X-ray diffraction (see Figure 2),[12] shows that the molybdenum atom displays a pseudo-octahedral coordination geometry.

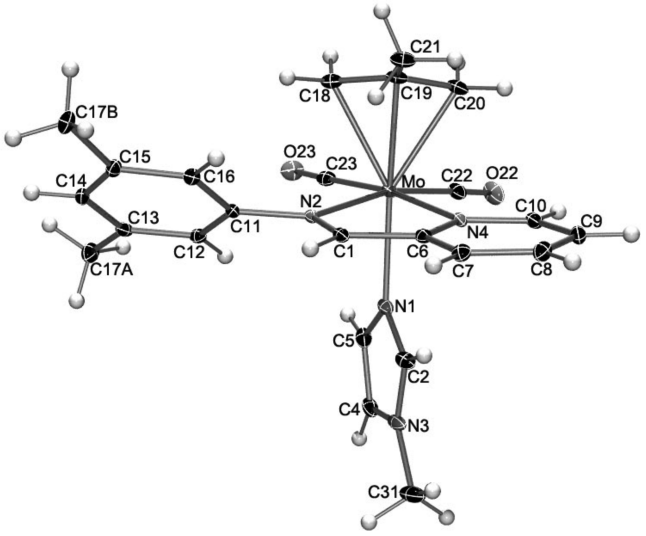

Figure 2. Molecular structure of the cation of compound **2c**.

The 2-pyridylimino chelate is coplanar with the two CO ligands, and the *N*-methylimidazole is *trans* to the η^3-allyl ligand. The pyridine and imine moieties of the new bidentate ligand are virtually coplanar reflecting conjugation, with the dihedral angle being 4.43°. The Mo–N(imidazole) bond distance, of 2.220(2) Å, is very close to that found for the only other crystallographically characterized *N*-alkylimidazole complex of the fragment {Mo(η^3-allyl)(CO)$_2$}, of 2.219(8) Å.[7]

The reaction of [Mo(η^3-C$_4$H$_7$)(CO)$_2$(*N*-MeIm)(py-2-CH=N-Ph)]OTf (**2a**) with a slight excess of KN(SiMe$_3$)$_2$ in THF at −78 °C afforded, as indicated by the large shift to lower wavenumbers of the ν_{CO} bands in the IR spectrum (from 1949, 1869 to 1932, 1835 cm^{-1}), the formation of a neutral species. The low stability of this deprotonated derivative precluded its isolation and, upon addition of trifluoromethanesulfonic acid in CH_2Cl_2, the stable compound **4a** was obtained as the main product of the reaction (Scheme 4). The IR ν_{CO} bands of the new compound **4a**, at 1950, 1969 cm^{-1}, indicated the protonation reaction had occurred and a cationic complex was formed.

The molecular structure of the cation of compound **4a**, determined by X-ray diffraction,[13] is depicted in Figure 3a showing that a tridentate N-donor ligand is now coordinated to the {Mo(η^3-methallyl)(CO)$_2$} fragment in a facial disposition. This tripodal ligand results from the C–C coupling between the central C atom of the imidazole (C2) and the imine C atom of the pyridylimino bidentante ligand (C1). The bond distance C1–C2, of 1.497(8) Å, is typical for a single C–C bond. Therefore, the C1 atom is sp^3 hybridized, the angles around it being consistent with an approximately tetrahedral geometry (C2–C1–N2 104.0(5)°, C6–C1–N2 110.9(5)°, C2–C1–C6 107.0(5)°). The C1–N2 bond distance is in agreement with a single bond (1.507(8) Å), whereas in the solid state structure of its precursor **2c** (determined by X-ray diffraction) this bond

Scheme 4. Reactivity of Cationic Imidazole 2-Pyridylimino Complexes 2a–e

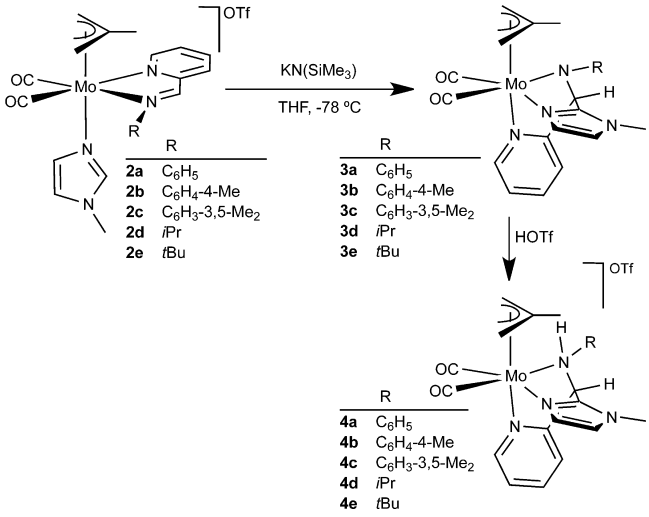

length was typical of a double bond (1.283(3) Å) as expected for an imine moiety. The originally imino nitrogen atom (N2) displays in **4a** a tetrahedral geometry, which is consistent with the protonation of this atom by the HOTf forming an amino group. The high quality of the results of the structural determination of compound **4a** allowed the hydrogen atom on N2 to be refined. Finally, it is interesting to note that in the solid state structure of the cationic complex of **4a** the pyridyl moiety is in *trans* disposition to the η^3-methallyl ligand, whereas in the starting compound (**2c**) the imidazole ligand is occupying this position. This indicates that the C–C coupling reaction is accompanied by a rotation of the trigonal face formed by the three nitrogen ligands, probably in order to minimize the steric hindrance in the resulting product.

The ^{1}H and ^{13}C NMR data in solution of the new compound **4a** are in accordance with the structure found in the solid state. The ^{1}H NMR spectrum undoubtedly shows the deprotonation of the imidazole central CH group (as only two signals at 7.17 and 6.90 ppm that correspond to imidazole CH moieties are observed), and the C–C coupling with the imine N=CH unit (as evidenced by the disappearance of the signal at 9.08 ppm assigned to that group in the ^{1}H NMR spectrum of **2a**). Moreover, the ^{1}H NMR spectrum of **4a** includes a singlet at 5.65 ppm that corresponds to the Csp^3–H group formed as a consequence of the C–C coupling reaction. Unfortunately, the signal of the new NH group is not observed, which can be attributed to the acidic character of this hydrogen. The ^{13}C NMR spectrum of **4a** corresponds to an asymmetric complex, showing for example two low intensity signals at 227.7 and 226.8 ppm for the two carbonyl ligands, and a signal at 64.3 ppm assigned to the new Csp^3 atom.

As we have discussed above, the solid state structure of compound **4a** showed that the formation of the tridentate ligand is accompanied by a rotation of the original N-donor ligands. Accordingly, the ^{1}H NMR spectra of **4a** in CD_2Cl_2 at variable temperature (from 298 to 213 K) showed the existence of a dynamic process. The data are in accordance with a trigonal twist rearrangement (that would involve a rotation of the triangular face formed by the tripodal ligand relative to the face formed by the allyl and the two carbonyl groups),[14] a process that has been frequently found for complexes of the fragment {Mo(η^3-allyl)(CO)$_2$}.[15,16]

DOI: 10.1021/ic502729z
Inorg. Chem. 2015, 54, 2580–2590

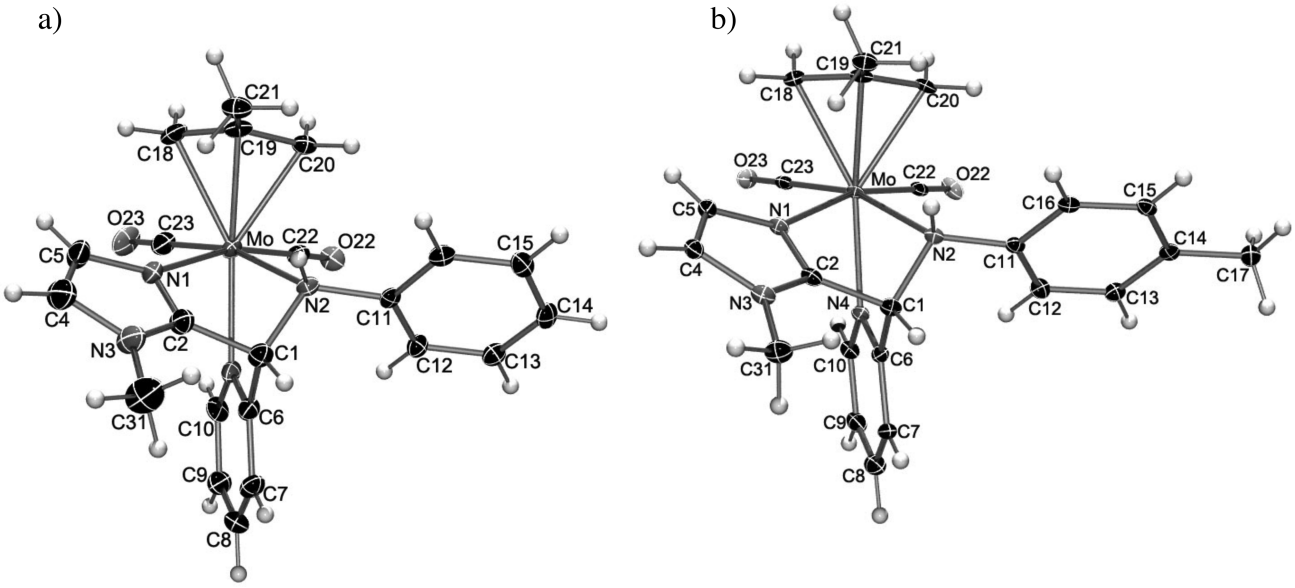

Figure 3. (a) Molecular structure of the cation of compound **4a**; (b) molecular structure of the cation of compound **4b**.

The reaction of the related compounds **2b** and **2c** toward the strong base $KN(SiMe_3)_2$ showed the same reactivity pattern discussed above for **2a**, but for these species the neutral derivatives, **3b** and **3c**, respectively (Scheme 4), could be isolated and characterized in solution by means of IR and ^1H NMR. The IR ν_{CO} bands, at approximately 20 cm^{-1} lower wavenumbers than those of the imidazole starting compounds, are typical of neutral complexes displaying a good σ-donor ligand (such as the deprotonated imidazole). The ^1H NMR spectra of **3b** and **3c** show characteristic features similar to those described for the spectrum of compound **4a**: i.e., only two N-MeIm CH groups are observed (two singlets at 7.02 and 6.19 ppm for **3b**), there is no longer an imine N═CH signal (at 9.03 ppm in the precursor **2b**), and instead there is a signal (at 5.76 ppm for **3b**) for the new Csp^3−H group originated as a consequence of the C(imidazolyl)−C(imine) bond formation. Unfortunately, the stability of complexes **3b** and **3c** was not enough to obtain the ^{13}C NMR spectra, as they decomposed after several hours in CD_2Cl_2 solution into a mixture of unidentified products.

The reaction of **3b** or **3c** intermediates with a slight excess of HOTf led to the formation of the cationic protonated products **4b** or **4c**, respectively (Scheme 4). The stability of the protonated products is considerably higher than that of the neutral species, which can be attributed to the presence of a highly reactive amido group[17] in **3b** or **3c** that, upon protonation, is transformed into a more stable amine moiety in **4b** or **4c**. The spectroscopic data of the new compounds are analogous to those of **4a**, and the solid state X-ray diffraction structures were determined for both compounds. In Figure 3b is depicted the molecular structure of the cation of **4b**,[18] showing the formation of the C−C coupling product. The central carbon atom of the N-MeIm moiety (C2) is therefore bonded to the imine carbon (C1), and the resulting tridentate ligand occupies one face of the octahedral coordination sphere of the molybdenum atom. The other face is occupied by the two CO ligands and the η^3-methallyl moiety.[14] As discussed for compound **4a**, the formation of the tridentate ligand implies a rotation of the N-donor ligands so that the 2-pyridyl group, and not the 2-imidazolyl, is *trans* to the methallyl ligand in **4b**.

After numerous attempts, only poor quality crystals were obtained for compound **4c**. The X-ray structure, although of low quality,[19] clearly shows that the connectivity of the molecule is analogous to those described previously for compounds **4a** and **4b**.

The ^1H NMR spectra of the crude of all the protonated compounds **4a**−**c** show the existence of two sets of signals attributed to the presence of two different diastereomers. The diastereomer that could be crystallyzed in each case was found to be the more abundant (for example in the case of the formation of **4b** the ratio of diasteromers is of 3.85). The existence of diasteromers is due to the presence of three stereocenters: the metal, the carbon atom that is the site of the nucleophilic attack, and the N atom that is protonated. As the stereochemistry of the metal and the C atom are prefixed by the geometry of the starting compounds, it is the final protonation step that leads to the formation of two diasteromers (each a pair of enantiomers). A NOESY experiment was carried out for compound **4a**, showing that the η^3-allyl ligand is oriented with its open face toward the carbonyl ligands, i.e. in the same orientation found in the solid state structures of compounds **4a**−**c**, and also found in its precursor **2a**.[11] This orientation of the η^3-allyl is the one most frequently found for complexes with the $\{Mo((\eta^3\text{-allyl})(CO)_2\}$fragment.[20]

Finally, to test the generality of the reactivity pattern previously described, we extended our study to alkyl- (instead of aryl-) amines in the Schiff condensation reaction. As a result, the pyridylimino bidentate ligands would be more electron rich, and therefore the nucleophilic attack onto the N═CH group of the imidazol-2-yl ligand would be less favorable.

Compounds $[Mo(\eta^3\text{-}C_4H_7)(CO)_2(N\text{-MeIm})(py\text{-}2\text{-}CH{=}N\text{-}R)]OTf$ (R= *i*Pr, **2d**; *t*Bu, **2e**) were prepared from the corresponding chloroderivatives (**1d** and **1e**) as described for compounds **2a**−**c** (see Scheme 3).[11] The addition of the equimolar amount of $KN(SiMe_3)_2$ to a previously cooled THF solutions of **2d** or **2e** afforded immediately the formation of neutral species resulting, presumably, from the deprotonation of the central CH group of the imidazole ligand. The subsequent addition of the electrophilic reagent HOTf led to more stable metal complexes,[21] **4d** and **4e**, respectively, that

DOI: 10.1021/ic502729z
Inorg. Chem. 2015, 54, 2580−2590

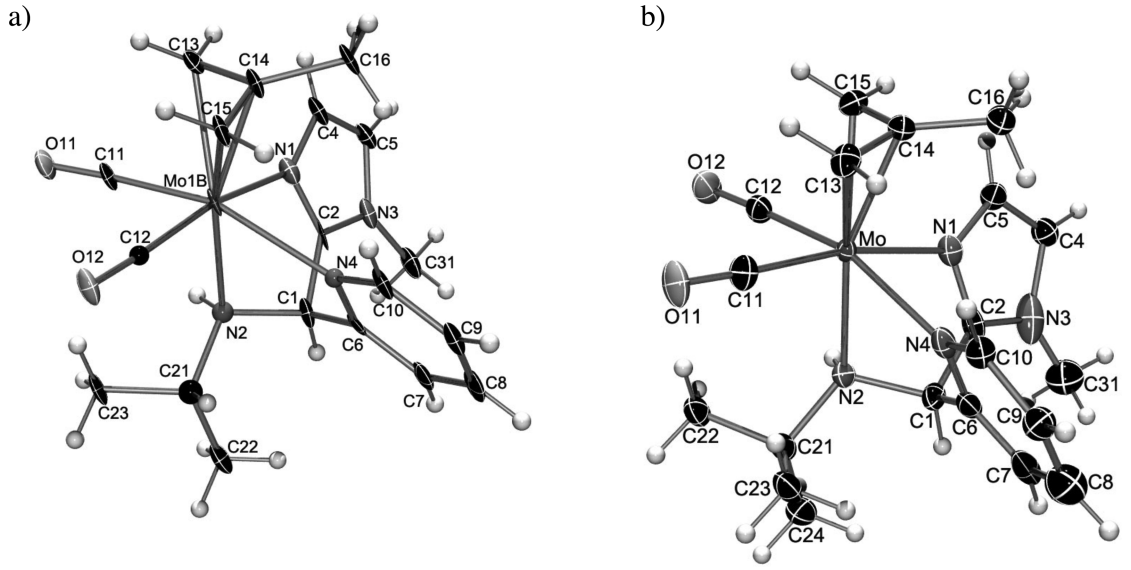

Figure 4. (a) Molecular structure of the cation of compound **4d**; (b) molecular structure of the cation of compound **4e**.

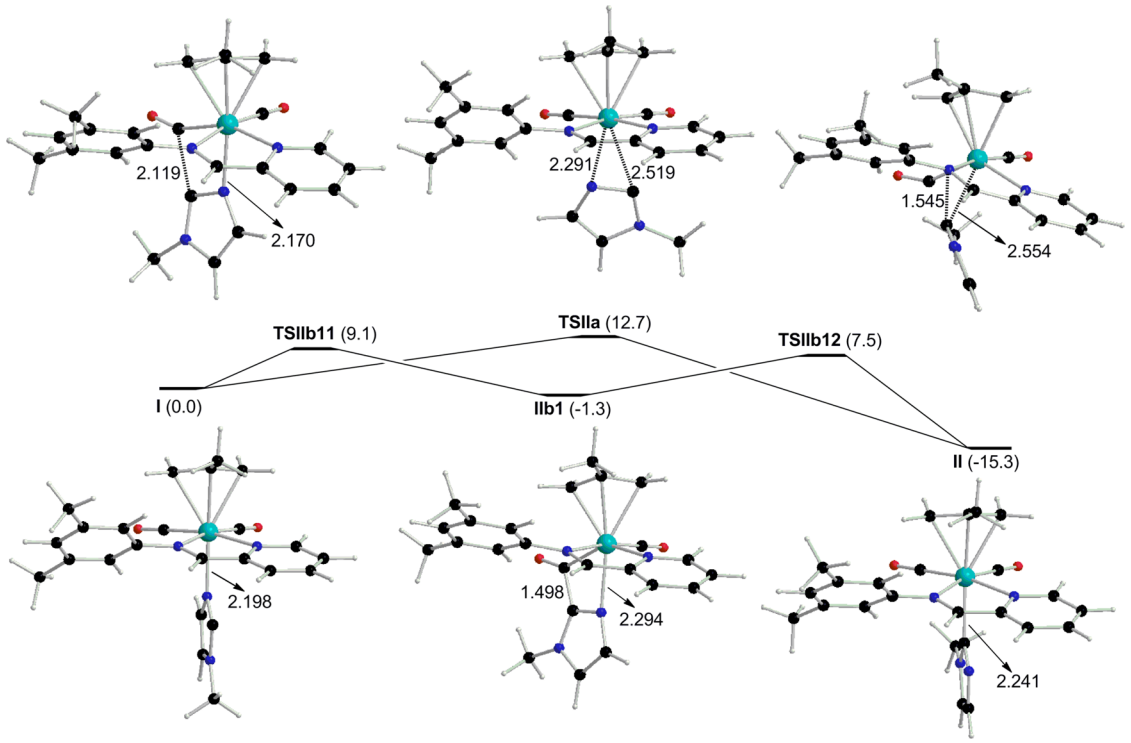

Figure 5. CPCM-B3LYP-D3/6-311++G(d,p) (LANL2DZ + *f* for Mo)//CPCM-B3LYP/6-31+G(d) (LANL2DZ + *f* for Mo) Gibbs energy profiles in THF solution of the mechanisms located for the formation of an imidazol-2-yl product starting from **I**. Relative Gibbs energies in THF solution, in kcal/mol, are given in parentheses. Most relevant distances are also included in angstroms.

were isolated and purified by crystallization. The more characteristic features of the NMR (^{1}H and ^{13}C) spectra of the new compounds are analogous to the pyridyliminoaryl compounds discussed above, and clearly indicate that (i) the strong base has deprotonated the central CH group of the *N*-methylimidazole ligand, and (ii) the generated nucleophile attacked the imine carbon atom to form a C—C bond, resulting in the formation of a nitrogen-donor tridentate ligand.[22] The solid state structures were determined by X-ray diffraction (Figure 4) and are in agreement with the structures proposed from the spectroscopic data in solution.[23,24]

A tridentate N-donor ligand, constituted by imidazolyl, pyridyl, and amine arms, is bonded in a facial disposition to the {Mo(η^3-methallyl)(CO)$_2$} fragment. The disposition of this ligand is different from that found in the aryl derivatives **4a**−**c**, since the amine function is *trans* to the allyl group. The fact that substituents *iso*-propyl and *tert*-butyl are notably bulkier than the aryl derivatives can explain this different orientation of the tripodal ligand.

To confirm that the C−C coupling reaction described in the present work proceeds through an intramolecular nucleophilic attack, a crossover experiment was conducted employing two

DOI: 10.1021/ic502729z
Inorg. Chem. 2015, 54, 2580−2590

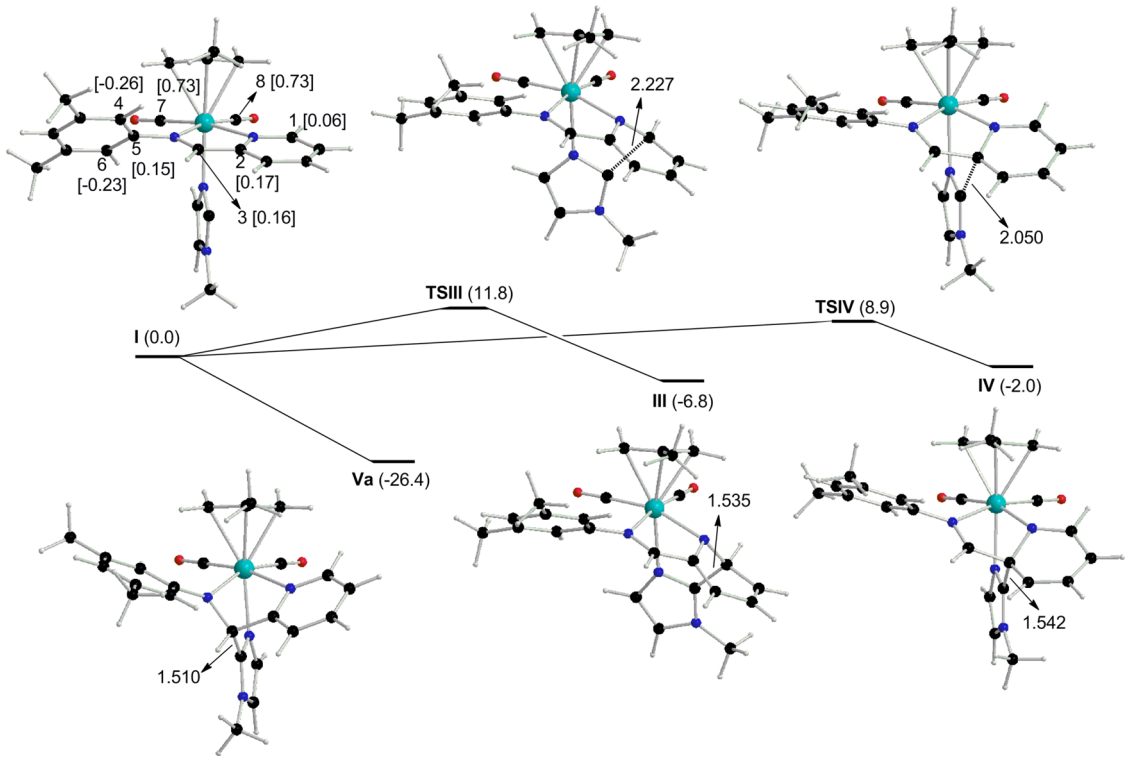

Figure 6. CPCM-B3LYP-D3/6-311++G(d,p) (LANL2DZ + *f* for Mo)//CPCM-B3LYP/6-31+G(d) (LANL2DZ + *f* for Mo) Gibbs energy profiles in THF solution of the mechanisms located for the formation of C−C coupling products starting from **I**. Relative Gibbs energies in THF solution (in kcal/mol) and NBO charges of the numbered atoms are given in parentheses and in square brackets, respectively. Most relevant distances are also included in angstroms.

complexes with different imines (*iso*-propyl vs *para*-tolyl) and different *N*-alkylimidazole ligands (methyl vs ethyl). The results showed that the only products obtained were those that resulted from an intramolecular reaction, with the cross-coupled products not being observed.[11]

DFT Computations. The deprotonation of $[Mo(\eta^3\text{-}C_4H_7)(bipy)(CO)_2(N\text{-}RIm)]OTf$ (R = Me, Mes) compounds leads to the formation of imidazol-2-yl species via the attack of the imidazole deprotonated carbon atom ($C_{imidazole}$) on a *cis*-CO ligand.[7] In contrast, the deprotonation of $[Mo(\eta^3\text{-}C_4H_7)(CO)_2(N\text{-MeIm})(py\text{-}2\text{-}CH{=}N\text{-}R')]OTf$ (R′ = C_6H_5 (**2a**), C_6H_4-4-Me (**2b**), C_6H_3-3,5-Me_2 (**2c**), *i*Pr (**2d**), *t*Bu (**2e**)) affords C—C coupling species. Furthermore, these products differ from the C—C coupling species obtained in the deprotonation of $[Re(CO)_3(bipy)(N\text{-RIm})]^+$ (R = Me, Mes) complexes.[7] In the rhenium compounds, the C—C coupling takes place between $C_{imidazole}$ and an *ortho* carbon atom of the bipy ligand, while in the present reaction it occurs between $C_{imidazole}$ and the imine carbon atom (C_{imine}) of the py-2-CH=N-R′ ligand. Aiming at understanding the reasons for the difference, we investigated the deprotonation of the $[Mo(\eta^3\text{-}C_4H_7)(CO)_2(N\text{-MeIm})(py\text{-}2\text{-}CH{=}N\text{-}R')]OTf$ complexes at the CPCM-B3LYP-D3/6-311++G(d,p) (LANL2DZ + *f* for Mo)//CPCM-B3LYP/6-31+G(d) (LANL2DZ + *f* for Mo) level of theory (see Computational Methods for details). Specifically, we first studied in detail the reaction mechanism for the Mo complex with R′ = C_6H_3-3,5-Me_2 (**2c** in Scheme 4). Next, we analyzed the influence of replacing this aryl group by *t*Bu (**2e** in Scheme 4) on the nature of the product.

As in previous studies,[6c,d,7] the deprotonated form of **2c** has been taken as the starting critical structure (**I** in Figures 5 and 6). The relative orientation of the ligands around the molybdenum center in **I** is analogous to that found in **2c**. Nonetheless, we also found an isomer of **I** (**Ii** in the Supporting Information) that differs from **2c** in having the central C atom of the N-MeIm (namely $C_{imidazole}$) pointing approximately toward the bisector of the angle defined by the two Mo−CO bonds, instead of toward the chelate ligand, as in **I** and **2c**. **Ii** is only 1.3 kcal/mol in Gibbs energy in THF solution more stable than **I**, and no TS was found for such an isomerization. As a consequence, hereafter, unless otherwise stated, Gibbs energies in THF solution will be referred to **I**.

First, we evaluated the generation of an imidazol-2-yl species. As previously found for related complexes,[7] this compound can be generated through two ways (see Figure 5). **I** can directly transform into the imidazol-2-yl product **II** (−15.3 kcal/mol) via the TS **TSIIa** (12.7 kcal/mol) in which $C_{imidazole}$ and the initially coordinated nitrogen atom interact simultaneously with the molybdenum center. Alternatively, **II** can be achieved through the attack of $C_{imidazole}$ onto each of the carbonyl ligands via a two-step pathway in both cases. The attack on the carbonyl ligand *trans* to the pyridyl group of the chelate ligand is found to be more favorable than the other; therefore, we only describe here that one for brevity (see the Supporting Information for the other carbonyl attack). The first step of this mechanism involves an energy jump of 9.1 kcal/mol controlled by the TS **TSIIb11** to afford the intermediate **IIb1** (−1.3 kcal/mol). In the second step, **IIb1** evolves into **II** via the TS **TSIIb12** (7.5 kcal/mol). As in related Mo and Re complexes,[7] the two-step mechanism is the one most favorable.

Next, we analyzed the formation of different C−C coupling species between $C_{imidazole}$ and the pyridylimine ligand (see Figure 6). The attack of $C_{imidazole}$ on the two *ortho* carbon atoms of the pyridine ring and the C_{imine} atom were studied (C1, C2,

DOI: 10.1021/ic502729z
Inorg. Chem. 2015, 54, 2580−2590

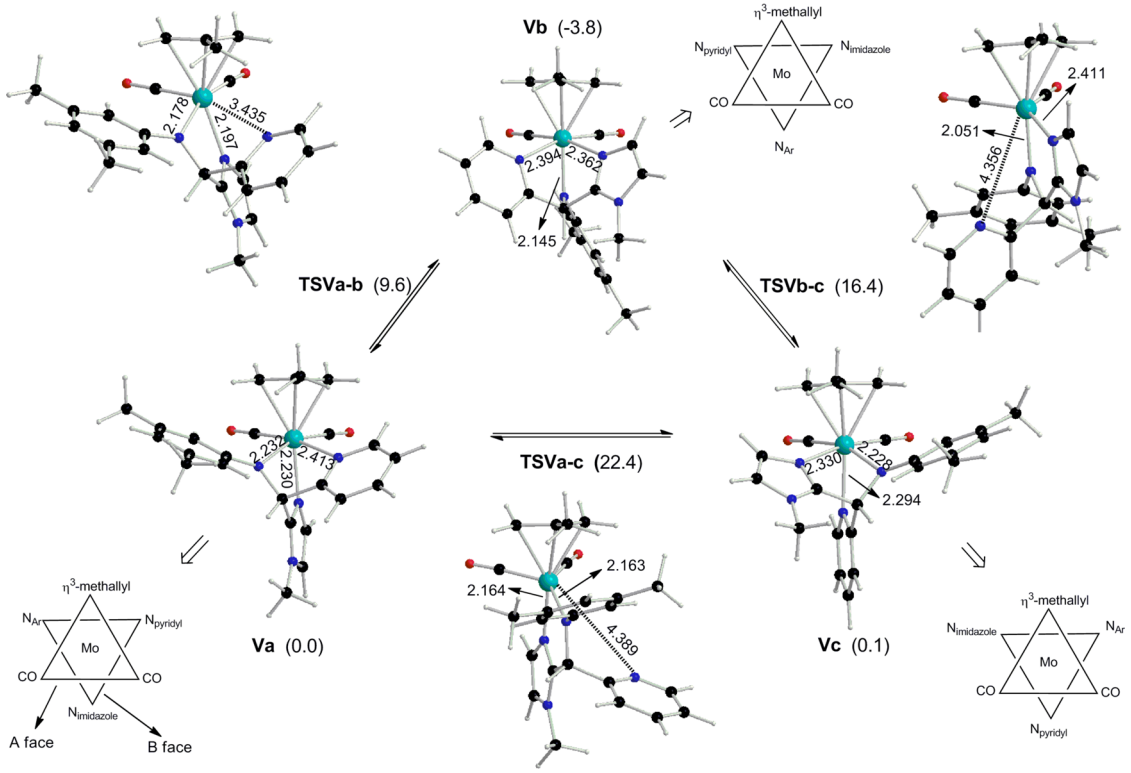

Figure 7. CPCM-B3LYP/6-31+G(d) (LANL2DZ + *f* for Mo) optimized structures of the different $C_{imidazole}$−C_{imine} coupling conformers formed for the C_6H_3-3,5-Me_2 derivative and the TS connecting them. CPCM-B3LYP-D3/6-311++G(d,p) (LANL2DZ + *f* for Mo)//CPCM-B3LYP/6-31+G(d) (LANL2DZ + *f* for Mo) Gibbs energies in THF solution referred to **Va** (in kcal/mol) are given in parentheses. Most relevant distances are also included in angstroms.

and C3, respectively in Figure 6). The formation of C−C coupling products between $C_{imidazole}$ and the *ipso* carbon atom and the *ortho* carbon atoms of the aryl ring (C5, C4, and C6, respectively, in Figure 6) was also considered, but as expected, they are notably less stable than those mentioned above (see the Supporting Information). As shown in Figure 6, the formation of the $C_{imidazole}$−C1 and $C_{imidazole}$−C2 coupling products (**III**, −6.8 kcal/mol, and **IV**, −2.0 kcal/mol, respectively) requires the surmounting of energy barriers of 11.8 (**TSIII**) and 8.9 (**TSIV**) kcal/mol, respectively. An NBO analysis of **I** reveals that C2 (0.17 *e*) has a larger positive atomic charge than C1 (0.06 *e*), which makes it more susceptible to a nucleophilic attack, and, consequently, **TSIV** is lower in energy than **TSIII**. The attack on the C_{imine} atom leads to the formation of a very stable $C_{imidazole}$−C_{imine} coupling species (**Va** in Figure 6, −26.4 kcal/mol). Unlike in the generation of **III** and **IV**, no TS was found for the formation of **Va** after an extensive search. This can be ascribed to the high reactivity of C_{imine} due to its electrophilic character (atomic charge of 0.16 *e* at **I**) combined with its ability to delocalize electron density toward the originally imine nitrogen atom, which in the C−C coupling product is part of an amido ligand.

Taking into account the previous discussion, we conclude that the generation of an imidazol-2-yl product (**II**) and of the $C_{imidazole}$−C1 (**III**) and $C_{imidazole}$−C2 (**IV**) coupling products is kinetically accessible as they show energy barriers of 9.1, 11.8, and 8.9 kcal/mol, respectively. However, the evolution of **I** to the $C_{imidazole}$−C_{imine} coupling product (**Va**) is even much more favorable due to the nonexistence of a kinetic barrier for such a molecular rearrangement, along with the fact that **Va** is a much more stable product. The transformation of **I** into **Va** involves the formation of a new C−C bond without any bond breaking, while the original Mo−$N_{imidazole}$ bond is replaced by the Mo−$C_{imidazole}$ bond for the process from **I** to **II**. This can explain the higher stability of **Va** compared to **II**. In addition, the generation of the $C_{imidazole}$−C_{imine} bond at **Va** does not require dearomatization of the pyridine ring, in contrast with what occurs when going from **I** to **III** or **IV**.

Despite the high stability of **Va** (−26.4 kcal/mol), this species can evolve into two isomers that are also very stable, **Vb** (−30.2 kcal/mol) and **Vc** (−26.3 kcal/mol) (see Figure 7). These three isomers present a pseudo-octahedral geometry. The two carbonyl ligands and the methallyl group occupy one triangular face of the pseudo-octahedron (hereafter denoted as A), while the other (henceforth referred as B) is determined by the tridentate N-donor ligand, consisting of imidazolyl, pyridyl, and amido arms (see for instance Va Figure 7). As in **2c** and **I**, **Va** has the imidazole group *trans* to the methallyl group, so the amido and pyridyl groups are both *trans* to the carbonyl ligands. In **Vb** and **Vc** the methallyl ligand is *trans* to the amido and pyridyl group, respectively, and hence, the N-donor groups are *trans* to the carbonyls. The interconversion between **Va**, **Vb**, and **Vc** could proceed via a trigonal-twist mechanism.[15] Starting from **Va**, a counterclockwise rotation of about 120° of B over A would lead to **Vb**, which in turn become **Vc** via another similar rearrangement. Alternatively, the clockwise rotation of B over A would directly transform **Va** into **Vc**. However, as shown in Figure 7, all the TSs (**TSVa-b**, **TSVb-c**, and **TSVa-c**) for the rearrangement of the tridentate ligand (**Va** → **Vb**, **Vb** → **Vc**, and **Va** → **Vc**, respectively) are pentacoordinated owing to the cleavage of the Mo−pyridyl bond. Accordingly, an NBO analysis of **Va** confirms that the Mo−$N_{pyridyl}$ bond is the

DOI: 10.1021/ic502729z
Inorg. Chem. 2015, 54, 2580−2590

weakest Mo−N interaction between Mo and the tridentate ligand. Specifically, the Mo−$N_{pyridyl}$ bond has a bond order of 0.3857 while values of 0.5169 and 0.5649 were found for the Mo−$N_{imidazole}$ and Mo−N_{imide} bonds, respectively. The breaking of one of the Mo−N bonds seems to be needed in order to favor the interconversion of the conformers containing the tridentate ligand rearrangement when bulky ligands are present in Mo complexes.[25] This could change in the absence of bulky ligands as reported in a theoretical study on octahedral vanadium complexes wherein no bond breaking was found at the TS located for trigonal twist.[26] Theoretical studies on this trigonal twist in molybdenum octahedral center are scarce,[25a] although it is common to attribute the dynamics deduced from variable-temperature NMR experiments to such processes.[27]

Concerning the energetics implied in the transformations **Va** → **Vb** → **Vc**, our results reveal Gibbs energy barriers of 9.6, 20.2, and 22.4 kcal/mol (measured from **Va**, **Vb**, and **Va**, respectively) for the interconversions **Va** → **Vb**, **Vb** → **Vc**, and **Va** → **Vc**, respectively. The highest energy barriers obtained are similar to those reported (∼22 kcal/mol) for a dissociative trigonal twist mechanism of other six-coordinate Mo complexes.[25a] Therefore, we conclude that **Va**, **Vb**, and **Vc** are continuously interconverting, and consequently, the complex should show a fluxional behavior. **Vb** is the most stable conformer in THF solution, but is only 3.8 and 3.9 kcal/mol more stable than **Va** and **Vc**, respectively. The protonation of these three stable conformers leads to the appearance of two diastereomers per deprotonated species, identified as **VxH** with **x** = **a**, **b**, **c**. As seen in Table 1, a diastereomer from **Vc**, (*RS*)-**VcH**, becomes slightly the most stable species. This isomer is also the one found in the solid state structure of **4c**, in which the pyridine ligand is *trans* to the methallyl group, and of the analogous complexes **4a** and **4b**.

Table 1. Relative Gibbs Energy, in kcal/mol, of the Different Diastereomers of the Protonated $C_{imidazole}$−C_{imine} Coupling Products Obtained from the Deprotonation of 2c and 2e at the CPCM-B3LYP-D3/6-311++G(d,p) (LANL2DZ + *f* for Mo)//CPCM-B3LYP/6-31+G(d) (LANL2DZ + *f* for Mo) Level of Theory[a]

	conformation **x** = **a**	conformation **x** = **b**	conformation **x** = **c**
(*RR*)-**VxH**	0.0	1.5	0.2
(*RS*)-**VxH**	0.7	2.1	−0.2
(*RR*)-**V′xH**	0.0	−1.0	5.5
(*RS*)-**V′xH**	7.7	−0.7	−0.4

[a]The most stable diastereomer in conformation **a** is taken as a reference in both cases.

On the basis of the results discussed above, it is also possible to rationalize the product obtained for the deprotonation of the *t*Bu-imine Mo complex (**2e** in Scheme 4). To that end, we focused our attention on the interconversion among the conformers analogous to **Va**, **Vb**, and **Vc** wherein the aryl group is replaced by *t*Bu (denoted as **V′a**, **V′b**, and **V′c**, respectively). As seen in Supporting Information Figure S3, the TSs for the transformations **V′a** → **V′b**, **V′b** → **V′c**, and **V′a** → **V′c** (**TSV′a-b**, **TSV′b-c**, and **TS′Va-c**, respectively) are analogous to those found for the aryl complexes. Concerning the energetics, **V′a** becomes **V′b** via a Gibbs energy barrier of 10.3 kcal/mol (**TSV′a-b**). A value of 21.5 kcal/mol (**TSV′b-c**) was found for the transformation **V′b** → **V′c** because **V′b** is 7.0 kcal/mol more stable than **V′a**. The interconversion **V′a** → **V′c** presents a Gibbs energy barrier still higher (28.5 kcal/mol, **TSV′a-c**). All these energy barriers are higher than those for the arylimino derivative, with differences in the 0.7−6.1 kcal/mol range. This can be mainly ascribed to the steric effect of the *t*Bu group. The results obtained for the *t*Bu-imino complex also suggest a fluxional dynamics between **V′a** and **V′b**, and between **V′b** and **V′c**, but not directly between **V′a** and **V′c**. Besides, the significant stability of **V′b** compared to **V′a** and **V′c** agrees with the finding of a solid state structure of a protonated complex (**4e**) with the *t*Bu-substituted nitrogen atom *trans* to the methallyl ligand (see Figure 4b). Accordingly, the analysis of the relative stability of the diastereomers derived from the protonation of **V′a**, **V′b**, and **V′c** confirms that the protonated conformers of **V′b**, (*RR*)-**V′bH** and (*RS*)-**V′bH**, are the most stable (see Table 1).

CONCLUSIONS

The reaction of the new cationic complexes of [Mo(η^3-C_4H_7)(CO)$_2$(*N*-MeIm)(py-2-CH═N-R)]OTf (R= C_6H_5, C_6H_4-4-Me, C_6H_3-3,5-Me_2, *i*Pr, *t*Bu) with the equimolar amount of the strong base KN($SiMe_3$)$_2$ at low temperature leads to the deprotonation of the central CH group of the *N*-methylimidazole ligand. The neutral species so formed are very reactive and immediately afford the C−C coupling products that result from the nucleophilic attack of the deprotonated imidazole C2 atom onto the imine CH moiety. The resulting N-donor tridentate ligand occupies one face of the pseudo-octahedral geometry of the complex, and its disposition depends on the nature of the substituent of the amine N atom. Whereas for aryl derivatives the pyridyl group is *trans* to the methallyl moiety, for the alkyl derivatives it is the amine function that occupies this position, probably in order to minimize steric congestion.

For this family of Mo(II) pyridylimino compounds the formation of the C−C coupling products is preferred over the formation of the imidazol-2-yl species, that had been previously found in the related 2,2′-bipyridine complexes [Mo(η^3-C_4H_7)(bipy)(CO)$_2$(N-RIm]OTf (R= Me, Mes). DFT calculations have shown, in agreement with the experimental results, that the formation of the C−C coupling product is undoubtedly the most favorable way of evolution of the deprotonated species, both kinetically (no TS was found for such molecular rearrangement) and thermodynamically (**Va** is 16.9 kcal/mol more stable than the 2-imidazolyl structure **II**). In that respect, the electrophilicity of the imine C atom along with its ability to delocalize electron density toward nitrogen are crucial.

EXPERIMENTAL SECTION

General. All manipulations were carried out under a nitrogen atmosphere using Schlenk techniques. Solvents were distilled from Na (toluene and hexanes), Na/benzophenone (THF), and CaH_2 (CH_2Cl_2). Compound [MoCl(η^3-C_4H_7)(CO)$_2$(NCMe)$_2$][28] was prepared as previously reported. Deuterated dichloromethane (Cambridge Isotope Laboratories, Inc.) was stored under nitrogen in a Young tube and used without further purification. ^{1}H NMR and ^{13}C NMR spectra were recorded on a Bruker Avance 300 or DPX-300 spectrometer. NMR spectra are referred to the internal residual solvent peak for ^{1}H and ^{13}C{^{1}H} NMR. IR solution spectra were obtained in a PerkinElmer FT 1720-X spectrometer using 0.2 mm CaF_2 cells. NMR samples were prepared under nitrogen using Kontes manifolds purchased from Aldrich. Full experimental details of all compounds are given in the Supporting Information, whereas herein only a set of

DOI: 10.1021/ic502729z
Inorg. Chem. 2015, 54, 2580−2590

complexes displaying each type of ligand (alkyl or aryl derivatives) is included as representative examples.

Crystal Structure Determination. *General Description.* For Compounds **1c**, **4a**, **4b**, and **4e**. Crystal data were collected on a Bruker APPEX II diffractometer using graphite-monochromated Mo Kα radiation (λ = 0.710 73 Å) from a fine-focus sealed tube source at 100 K. Computing data and reduction were made with the APPEX II software.[29] In all cases empirical absorption corrections were applied using SADABS.[30] For compound **4e**: data collection was performed at 150 K on an Oxford Diffraction Xcalibur Nova single crystal diffractometer, using Cu Kα radiation (λ= 1.5418 Å). Images were collected at a 65 mm fixed crystal-detector distance, using the oscillation method, with 1° oscillation and variable exposure time per image (4−16 s). Data collection strategy was calculated with the program CrysAlis^{Pro} CCD.[31] Data reduction and cell refinement was performed with the program CrysAlis^{Pro} RED.[31] An empirical absorption correction was applied using the SCALE3 ABSPACK.[31] In all cases the structures were solved using SIR92[32] and finally refined by full-matrix, least-squares based on F^2 by SHELXL.[33] Molecular graphics were made with ORTEP 3.[34]

Computational Methods. Quantum chemical computations were carried out with the Gaussian 09 series of programs.[35] Full geometry optimizations of stable species and TS were performed in THF solution from the outset with the Conductor-like Polarizable Continuum Model (CPCM)[36] and the Universal Force Field (UFF) radii[37] in conjunction with the hybrid density functional B3LYP[38] and the 6-31+G(d)[39] basis set for nonmetal atoms together with the LANL2DZ[40] with *f* polarization functions[41] of exponent 1.043 for Mo and by using the standard Schlegel's algorithm.[42] A relative permittivity of 7.58 was assumed in the calculations to simulate THF as the solvent experimentally used for all the cases. To further refine the quality of the above-mentioned energies, we also performed single-point CPCM-B3LYP/6-311++G(d,p)[39] (LANL2DZ + *f* for Mo) and B3LYP-D3[43] dispersion calculations on the CPCM-B3LYP/6-31+G(d) geometries. For the latter computations, we used the Becke−Johnson damping function[44] to avoid near singularities for small interatomic distances. The nature of the stationary points was verified by analytical computations of harmonic vibrational frequencies. Intrinsic reaction coordinate (IRC) calculations with the Gonzalez and Schlegel method[45] were carried out to check the two minimum energy structures connecting each TS except for the species involved in the trigonal twist mechanism. The complexity of these molecular rearrangements prevented the use of the IRC algorithm; we instead analyzed the transition vector to verify the TS connectivity. Besides this, we also checked how the TS was finally reached from an initial geometry wherein the methallyl ligand is in front of the pyridyl ligand, the imidazole ligand, or the nitrogen atom bearing the Ar or *t*Bu group. Thermodynamic magnitudes (Δ*H*, Δ*S*, and Δ*G*) were also calculated within the ideal gas, rigid rotor, and harmonic oscillator approximations at a pressure of 1 atm and a temperature of 195.15 K.[46] For interpretation purposes, a natural bond orbital (NBO) analysis was also performed.[47]

*Synthesis of [MoCl(η^3-C_4H_7)(CO)$_2$(py-2-CH═N−C_6H_4-4-Me)] (**1b**).* Pyridine-2-carboxaldehyde (29 μL, 0.308 mmol) and *p*-toluidine (0.033 g, 0.308 mmol) were added to a solution of [MoCl(η^3-C_4H_7)(CO)$_2$(NCMe)$_2$] (0.100 g, 0.308 mmol) in THF (20 mL), and the reaction mixture was stirred for 30 min. The solvent was evaporated under reduced pressure to dryness, and the resulting violet powder was washed with hexane (2 × 20 mL) and dried under vacuum. Compound **1b** was obtained as a violet powder. Yield: 105 mg (78%). IR (CH_2Cl_2, cm^{-1}): 1951, 1875 (ν_{CO}). ^{1}H NMR (CD_2Cl_2): δ 8.79 (m, 1H, py), 8.42 (s, 1H, N═C*H*), 7.99 (m, 1H, py), 7.87 (m, 1H, py), 7.54 (m, 1H, py), 7.38 (d (*J* = 8.2), 2H, C_6H_4), 7.29 (d (*J* = 8.2), 2H, C_6H_4), 2.78 (m, 1H, H_{syn} η^3-C_4H_7), 2.41 (s, 3H, CH_3 C_6H_4-4-Me), 2.30 (m, 1H, H_{syn} η^3-C_4H_7), 1.35 (s_{br}, 4H, CH_3 and H_{anti} η^3-C_4H_7), 1.11 (s, 1H, H_{anti} η^3-C_4H_7). ^{13}C{^{1}H} NMR (CD_2Cl_2): δ 227.1, 226.8 (CO), 162.5 (N═CH), 153.6, 152.3, 148.7, 139.9, 138.8, 130.4, 129.3, 127.5, 122.4 (py-2-CH═N—C_6H_5), 83.8 (C_2 η^3-C_4H_7), 54.2, 52.7 (C_1 and C_3 η^3-C_4H_7), 23.2 (CH_3 C_6H_4-4-Me), 19.3 (CH_3 η^3-C_4H_7). Anal. Calcd for $C_{19}H_{19}ClMoN_2O_2$: C 52.01, H 4.36, N 6.38. Found: C 51.98, H 4.32, N 6.18.

*Synthesis of [MoCl(η^3-C_4H_7)(CO)$_2$(py-2-CH═N-tBu)] (**1e**).* Compound **1e** was prepared as described above for compound **1b**, starting from [MoCl(η^3-C_4H_7)(CO)$_2$(NCMe)$_2$] (100 mg, 0.308 mmol), pyridine-2-carboxaldehyde (29 μL, 0.308 mmol), and tertbutylamine (32 μL, 0.308 mmol). Compound **1e** was obtained as a dark blue solid. Yield: 161 mg (87%). IR (CH_2Cl_2, cm^{-1}): 1949, 1864 (ν_{CO}). ^{1}H NMR (CD_2Cl_2): δ 8.76 (m, 1H, py), 8.54 (s, 1H, N═C*H*), 8.01 (m, 1H, py), 7.81 (m, 1H, py), 7.54 (m, 1H, py), 3.13 (m, 1H, H_{syn} η^3-C_4H_7), 2.77 (s_{br}, 1H, H_{syn} η^3-C_4H_7), 1.59 (s, 9H, *t*Bu), 1.34 (s, 3H, CH_3 η^3-C_4H_7), 1.31 (s, 1H, H_{anti} η^3-C_4H_7), 1.27 (s, 1H, H_{anti} η^3-C_4H_7). ^{13}C{^{1}H} NMR (CD_2Cl_2): δ 228.3, 227.1 (CO), 163.9 (N═CH), 154.1, 151.6, 138.6, 128.8, 127.2 (py), 83.4 (C_2 η^3-C_4H_7), 70.8 (*t*Bu), 64.0 (C_1 or C_3 η^3-C_4H_7), 32.5 (CH_3 *t*Bu), 19.1 (CH_3 η^3-C_4H_7). The signal of C_1 or C_3 of the methallyl ligand is overlapped with the solvent residual. Anal. Calcd for $C_{16}H_{21}ClMoN_2O_2$: C 47.48, H 5.23, N 6.92. Found: C 47.49, H 4.99, N 6.83.

*Synthesis of [Mo(η^3-C_4H_7)(CO)$_2$(N-MeIm)(py-2-CH═N—C_6H_4-4-Me)]OTf (**2b**).* To a solution of [MoCl(η^3-C_4H_7)(CO)$_2$(py-2-CH═N—C_6H_4-4-Me)] (**1b**) (50 mg, 0.114 mmol) in CH_2Cl_2 (20 mL) were added AgOTf (35 mg, 0.136 mmol) and MeCN (3 mL), and the mixture was stirred in the dark for 1 h. The resulting slurry was filtered off the white solid (AgCl), and the solvent was evaporated to dryness. The dark red residue was redissolved in CH_2Cl_2 (20 mL), *N*-MeIm (10 μL, 0.125 mmol) was added, and the reaction mixture was allowed to stir for 1 h. The solvent was concentrated under reduced pressure to a volume of 7−10 mL, and addition of hexane (15 mL) caused the precipitation of a dark red solid, which was washed with hexane (2 × 20 mL) and dried under vacuum. Yield: 63 mg (87%). IR (CH_2Cl_2, cm^{-1}): 1951, 1869 (ν_{CO}). ^{1}H NMR (CD_2Cl_2): δ 9.05 (s, 1H, N═C*H*), 8.77 (m, 1H, py), 8.41 (m, 1H, py), 8.16 (m, 1H, py), 7.61 (m, 1H, py), 7.43 (s, 1H, NC*H*N), 7.31 (d (*J* = 8.4), 2H, C_6H_4), 7.25 (d (*J* = 8.4), 2H, C_6H_4), 7.10 (s_{br}, 1H, C*H* *N*-MeIm), 6.97 (s_{br}, 1*H*, C*H* *N*-MeIm), 3.65 (s, 3H, CH_3 *N*-MeIm), 3.05 (m, 1H, H_{syn} η^3-C_4H_7), 2.59 (m, 1H, H_{syn} η^3-C_4H_7), 2.42 (s, CH_3 C_6H_4-4-Me), 1.59 (s, 1H, H_{anti} η^3-C_4H_7), 1.34 (s_{br}, 4H, CH_3 and H_{anti} η^3-C_4H_7). ^{13}C{^{1}H} NMR (CD_2Cl_2): δ 226.0, 225.8 (CO), 166.1 (N═CH), 153.8, 152.4, 147.3, 141.1, 140.6, 139.9, 132.0, 130.9, 128.9, 122.9, 122.7 (py-2-CH═N—C_6H_4-4-Me and *N*-MeIm), 86.1 (C_2 η^3-C_4H_7), 58.1, 56.3 (C_1 and C_3 η^3-C_4H_7), 35.2 (CH_3 *N*-MeIm), 21.4 (CH_3 C_6H_4-4-Me), 18.9 (CH_3 η^3-C_4H_7). Anal. Calcd for $C_{24}H_{25}F_3MoN_4O_5S$: C 45.43, H 3.97, N 8.83. Found: C 45.91, H 4.06, N 8.96.

*Synthesis of [Mo(η^3-C_4H_7)(CO)$_2$(N-MeIm)(py-2-CH═N-tBu)]OTf (**2e**).* Compound **2e** was prepared following the procedure described for the synthesis of **2b**, starting from [MoCl(η^3-C_4H_7)(CO)$_2$(py-2-CH═N-*t*Bu)] (**1e**) (50 mg, 0.124 mmol), AgOTf (35 mg, 0.136 mmol), and *N*-MeIm (10 μL, 0.125 mmol). Compound **2e** was obtained as a dark red microcrystalline solid. Yield: 64 mg (87%). IR (CH_2Cl_2, cm^{-1}): 1947, 1864 (ν_{CO}). ^{1}H NMR (CD_2Cl_2): δ 8.97 (s, 1H, N═C*H*), 8.67 (m, 1H, py), 8.38 (m, 1H, py), 8.22 (m, 1H, py), 7.64 (m, 1H, py), 7.22 (s, 1H, NC*H*N), 6.98 (s_{br}, 1H, C*H* *N*-MeIm), 6.91 (s_{br}, 1*H*, C*H* *N*-MeIm), 3.68 (s, 3H, CH_3 *N*-MeIm), 3.42 (m, 1H, H_{syn} η^3-C_4H_7), 2.94 (m, 1H, H_{syn} η^3-C_4H_7), 1.62 (s, 1H, H_{anti} η^3-C_4H_7), 1.42 (s, 1H, H_{anti} η^3-C_4H_7), 1.38 (s, 9H, CH_3 *t*Bu), 1.23 (s, 3H, CH_3 η^3-C_4H_7). ^{13}C{^{1}H} NMR (CD_2Cl_2): δ 227.1, 226.2 (CO), 166.8 (N═CH), 154.5, 151.7, 140.6, 140.3, 131.8, 131.1, 128.6, 122.4 (py-2-CH═N-*t*Bu and *N*-MeIm), 86.5 (C_2 η^3-C_4H_7), 64.9 (*t*Bu), 58.7, 56.2 (C_1 and C_3 η^3-C_4H_7), 34.9 (CH_3 *N*-MeIm), 31.9 (CH_3 *t*Bu), 18.6 (CH_3 η^3-C_4H_7). Anal. Calcd for $C_{21}H_{27}F_3MoN_4O_5S$: C 42.00, H 4.53, N 9.33. Found: C 41.81, H 4.87, N 9.02.

*Reaction of [Mo(η^3-C_4H_7)(CO)$_2$(N-MeIm)(py-2-CH═N—C_6H_4-4-Me)]OTf (**2b**) with KN(SiMe$_3$)$_2$. Synthesis of **3b**.* KN(SiMe$_3$)$_2$ (0.15 mL of a 0.5 M solution in toluene, 0.076 mmol) was added to a solution of compound **2b** (40 mg, 0.063 mmol) in THF (15 mL), previously cooled to −78 °C. The color of the solution changed immediately from dark red to orange, and the solvent was evaporated to dryness under reduced pressure. The residue was extracted with CH_2Cl_2 (20 mL) and filtered via canula, and the resulting solution was concentrated to a volume of 5 mL. Addition of hexane (15 mL) caused

DOI: 10.1021/ic502729z
Inorg. Chem. 2015, 54, 2580−2590

the precipitation of a dark yellow solid that was washed with hexane (2 × 15 mL). Yield: 19 mg (63%). IR (CH_2Cl_2, cm^{-1}): 1929, 1833 (ν_{CO}). ^1H NMR (CD_2Cl_2): δ 8.57 (m, 1H, py), 7.77 (m, 1H, py), 7.53 (m, 1H, py), 7.17 (m, 1H, py), 6.95 (m, 5H, C_6H_4 and C*H* *N*-MeIm), 6.71 (s_{br}, 1H, C*H* *N*-MeIm), 5.72 (s, 1*H*, Csp^{3}H), 3.71 (s, 3H, CH_3 *N*-MeIm), 3.31 (m, 2H, H_{syn} η^3-C_4H_7), 2.20 (s, CH_3 C_6H_4-4-Me), 1.90 (s, 3H, CH_3 η^3-C_4H_7) 1.24 (s, 1H, H_{anti} η^3-C_4H_7), 1.08 (s, 1H, H_{anti} η^3-C_4H_7). Anal. Calcd for $C_{23}H_{24}MoN_4O_2$: C 57.03, H 4.99, N 11.57. Found: C 57.26, H 4.66, N 2.13.

Reaction of ***3b*** *with HOTf. Synthesis of* ***4b****.* HOTf (8 μL, 0.091 mmol) was added to a solution of compound **3b** (0.040 g, 0.083 mmol) in CH_2Cl_2, and the reaction mixture was stirred for 15 min at room temperature. The solvent was evaporated to a volume of 5 mL, and addition of hexane caused the precipitation of a red solid which was washed with hexane (2 × 15 mL). Slow diffusion of hexane (15 mL) into a concentrated solution of **4b** in CH_2Cl_2 (5 mL) afforded red crystals, one of which was employed for an X-ray structure determination. Yield: 36 mg (69%). IR (KBr, cm^{-1}): 3456 (ν_{NH}), 1947, 1858 (ν_{CO}). IR (CH_2Cl_2, cm^{-1}): 1949, 1860 (ν_{CO}). ^1H NMR (CD_2Cl_2): δ 9.66 (m, 1H, py), 8.03 (m, 1H, py), 7.71 (m, 1H, py), 7.57 (m, 1H, py), 7.20 (s, 1H, C*H* *N*-MeIm), 7.05 (d (J = 8.2), 2H, C_6H_4), 6.93 (s, 1H, C*H* *N*-MeIm), 6.87 (d (J = 8.2), 2H, C_6H_4), 5.64 (s, 1*H*, Csp^{3}H), 3.81 (s, 3H, CH_3 *N*-MeIm), 3.53 (m, 1H, H_{syn} η^3-C_4H_7), 2.71 (m, 1H, H_{syn} η^3-C_4H_7), 2.31 (s, CH_3 C_6H_4-4-Me), 1.98 (s, 3H, CH_3 η^3-C_4H_7), 1.52 (s, 1H, H_{anti} η^3-C_4H_7), 1.31 (s, 1H, H_{anti} η^3-C_4H_7). $^{13}C\{^1H\}$ NMR (CD_2Cl_2): δ 227.7, 226.9 (CO), 156.7, 146.9, 142.1, 141.8, 137.7, 130.6, 130.3, 127.8, 126.2, 124.2, 123.4, 122.7 (py-2-CH=N—C_6H_4-4-Me and *N*-MeIm), 85.5 (C_2 η^3-C_4H_7), 64.5 (Csp^3), 58.0 (C_1 or C_3 η^3-C_4H_7), 34.8 (CH_3 *N*-MeIm), 20.8, 20.6 (CH_3 C_6H_4-4-Me and η^3-C_4H_7). The signal of C_1 or C_3 of the methallyl ligand is overlapped with the solvent residual peak. Anal. Calcd for $C_{24}H_{25}F_3MoN_4O_5S$: C 45.43, H 3.97, N 8.83. Found: C 45.76, H 4.10, N 9.05.

Reaction of [Mo(η^3-C_4H_7)(CO)$_2$(N-MeIm)(py-2-CH=N-tBu] ***(2e)*** *with KN(SiMe$_3$)$_2$ Followed by Addition of HOTf. Synthesis of* ***4e****.* $KN(SiMe_3)_2$ (0.200 mL of a 0.5 M solution in toluene, 0.100 mmol) was added to a solution of compound **2e** (50 mg, 0.083 mmol) in THF (20 mL) cooled to −78 °C. The reaction mixture was allowed to reach room temperature and stirred for 40 min. The solvent was evaporated to dryness, the residue was extracted with CH_2Cl_2 (20 mL), and HOTf (9 μL, 0.101 mmol) was added. After 15 min stirring at room temperature the reaction mixture was filtered via canula, the solvent evaporated under reduced pressure, and the resulting yellow solid was washed with hexane (2 × 20 mL) and dried under vacuum. Yield: 31 mg (62%). IR (KBr, cm^{-1}): 3451 (ν_{NH}), 1945, 1856 (ν_{CO}). IR (CH_2Cl_2, cm^{-1}): 1950, 1861 (ν_{CO}). ^1H NMR (CD_2Cl_2): δ 9.07 (m, 1H, py), 7.97 (m, 1H, py), 7.81 (m, 1H, py), 7.50 (m, 1H, py), 7.16 (s, 1H, C*H* *N*-MeIm), 6.90 (s, 1*H*, C*H* *N*-MeIm), 5.71 (s, 1H, Csp^{3}H), 4.56 (s_{br}, 1H, N*H*), 3.83 (s, 3H, CH_3 *N*-MeIm), 3.50 (m, 1H, H_{syn} η^3-C_4H_7), 3.45 (m, 1H, H_{syn} η^3-C_4H_7), 1.80 (s, 3H, CH_3 η^3-C_4H_7), 1.44 (s_{br}, 1H, H_{anti} η^3-C_4H_7), 1.35 (s_{br}, 10H, *t*Bu and H_{anti} η^3-C_4H_7). $^{13}C\{^1H\}$ NMR (CD_2Cl_2): δ 222.7, 226.9 (CO), 156.0, 152.9, 146.9, 141.7, 127.3, 125.5, 124.1, 123.4 (py-2-CH=N-*t*Bu), 83.1 (C_2 η^3-C_4H_7), 60.0, 56.1 (C_1 and C_3 η^3-C_4H_7), 57.7 (Csp^3), 35.0 (CH_3 *N*-MeIm), 29.6 (CH_3 *t*Bu), 19.1 (CH_3 η^3-C_4H_7). Anal. Calcd for $C_{21}H_{27}F_3MoN_4O_5S$: C 42.00, H 4.53, N 9.33. Found: C 42.11, H 4.69, N 8.97.

■ ASSOCIATED CONTENT

Supporting Information

Full experimental details for all compounds, X-ray crystallographic data for compounds **2c** and **4a**, **4b**, **4d**, and **4e** in CIF format, discussion about the mechanisms not included in the paper, and full DFT details. This material is available free of charge via the Internet at http://pubs.acs.org

■ AUTHOR INFORMATION

Corresponding Authors

*E-mail: jdal@unex.es.
*E-mail: rlopez@uniovi.es.
*E-mail: l.riera@cinn.es.

Notes

The authors declare no competing financial interest.

■ ACKNOWLEDGMENTS

Financial support from the Ministerio de Economía y Competitividad (Projects CTQ2010-18231, CTQ2012-37370-C02-01, and CTQ2012-37370-C02-02) is gratefully acknowledged. J.D. thanks the Fundación Computación y Tecnologías Avanzadas de Extremadura (COMPUTAEX) for computing resources.

■ REFERENCES

(1) This subject has been the topic of several reviews, see for example: (a) SóvÁGÓ, I.; Várnagy, K.; Ösz, K. *Comments Inorg. Chem.* **2002**, *23*, 149−178. (b) Gaggelli, E.; Kozlowsky, H.; Valensin, D.; Valensin, G. *Chem. Rev.* **2006**, *106*, 1995−2044. (c) Faller, P.; Hureau, C. *Dalton Trans.* **2009**, 1080−1094.

(2) (a) Sundberg, R. J.; Martin, R. B. *Chem. Rev.* **1974**, *74*, 471−517. (b) Reedijk, J. In *Comprehensive Coordination Chemistry*; Wilkinson, G., Gillard, R. D., McCleverty, J. A., Eds.; Pergamon Press: Oxford, U.K., 1984; Vol. *2*, pp 73−98.

(3) (a) Gillard, R. D. *Comments Inorg. Chem.* **1986**, *5*, 175−199. (b) Praetorius, J. M.; Wang, R.; Crudden, C. M. *Organometallics* **2010**, *29*, 554−561.

(4) See, for example: (a) Hahn, F. E.; Jahnke, M. C. *Angew. Chem., Int. Ed.* **2008**, *47*, 3122−3172. (b) Jahnke, M. C.; Hahn, F. E. *Top. Organomet. Chem.* **2010**, *30*, 95−129.

(5) As far as we know, prior to our work there are just a couple of examples of this type of reaction: (a) Müller, J.; Stock, R. *Angew. Chem., Int. Ed.* **1983**, *22*, 993−993. (b) Ruiz, J.; Perandones, B. F. *J. Am. Chem. Soc.* **2007**, *129*, 9298−9299.

(6) (a) Huertos, M. A.; Pérez, J.; Riera, L. *J. Am. Chem. Soc.* **2008**, *130*, 5662−5663. (b) Huertos, M. A.; Pérez, J.; Riera, L.; Menéndez-Velázquez, A. *J. Am. Chem. Soc.* **2008**, *130*, 13530−13531. (c) Huertos, M. A.; Pérez, J.; Riera, L.; Díaz, J.; López, R. *Angew. Chem., Int. Ed.* **2010**, *49*, 6409−6412. (d) Huertos, M. A.; Pérez, J.; Riera, L.; Díaz, J.; López, R. *Chem.—Eur. J.* **2010**, *16*, 8495−8507. (e) Huertos, M. A.; Pérez, J.; Riera, L. *Chem.—Eur. J.* **2012**, *18*, 9530−9533. (e) Viguri, M. E.; Huertos, M. A.; Pérez, J.; Riera, L.; Ara, I. *J. Am. Chem. Soc.* **2012**, *134*, 20326−20329. (f) Viguri, M. E.; Huertos, M. A.; Pérez, J.; Riera, L. *Chem.—Eur. J.* **2013**, *19*, 12974−12977.

(7) Brill, M.; Díaz, J.; Huertos, M. A.; López, R.; Pérez, J.; Riera, L. *Chem.—Eur. J.* **2011**, *17*, 8584−8595.

(8) Dominey, R. N.; Hauser, B.; Hubbard, J.; Dunham, J. *Inorg. Chem.* **1991**, *30*, 4754−4758.

(9) (a) Herrick, R. S.; Houde, K. L.; McDowell, J. S.; Kiczek, L. P.; Bonavia, G. *J. Organomet. Chem.* **1999**, *589*, 29−37. (b) Herrick, R. S.; Wrona, I.; McMicken, N.; Jones, G.; Ziegler, C. J.; Shaw, J. *J. Organomet. Chem.* **2004**, *689*, 4848−4855. (c) García-Rodríguez, R.; Miguel, D. *Dalton Trans.* **2006**, 1218−1225. (d) Miguel, D.; García-Escudero, L. A.; Turiel, J. A. *J. Organomet. Chem.* **2006**, *691*, 3434−3444.

(10) (a) Alberto, R.; Wang, W.; Spingler, B. *Inorg. Chim. Acta* **2003**, *355*, 386−393. (b) Miguel, D.; Álvarez, C. M.; García-Rodríguez, R. *Dalton Trans.* **2007**, 3546−3554.

(11) See Supporting Information for further experimental details.

(12) Selected crystallographic data for **2c**: $C_{25}H_{27}F_3MoN_4O_5RS$, M = 648.51, monoclinic, $P2_1/c$, a = 10.890(5) Å, b = 17.561(5) Å, c = 14.168(5) Å, α = 90°, β = 93.464(5)°, γ = 90°, 100.0(1) K, V = 2704(2) Å^3, Z = 4. 5335 reflections measured, 5145 independent (R_{int} = 0.0275). R1 = 0.0289, wR2 = 0.0762 (all data).

DOI: 10.1021/ic502729z
Inorg. Chem. 2015, 54, 2580−2590

(13) Selected crystallographic data for **4a**: $C_{23}H_{23}F_3MoN_4O_5S\cdot CH_2Cl_2$, M = 705.38, monoclinic, $P2_1/c$, a = 8.519(5) Å, b = 11.186(5) Å, c = 30.020(5) Å, α = 90°, β = 93.456(5)°, γ = 90°, 100.0(1) K, V = 2856(2) Å^3, Z = 4. 7087 reflections measured, 6136 independent (R_{int} = 0.0470). R1 = 0.0511, wR2 = 0.1306 (all data).
(14) In these complexes it is customary to describe the structures considering that the η^3-allyl ligand occupies one coordination site, see for example: (a) Brisdon, B. J. *J. Organomet. Chem.* **1977**, *125*, 225−230. (b) Brisdon, B. J.; Woolf, A. A. *J. Chem. Soc., Dalton Trans.* **1978**, 291−295.
(15) Faller, J. W.; Haitko, D. A.; Adams, R. D.; Chodosh, D. F. *J. Am. Chem. Soc.* **1979**, *101*, 865−876.
(16) It has to be noted that for the starting compound [Mo(η^3-C_4H_7)(CO)$_2$(*N*-RIm)(py-2-CH═N-Ph)]OTf (**2a**) the NMR dynamic process is not observed in CD_2Cl_2 at low temperature (198 K). This behavior is similar to that of related allyldicarbonyl molybdenum(II) complexes with diimine chelate ligands, such as 2,2′-bipyridine or 1,10-phenanthroline, see: Davis, R.; Kane-Maguire, L. A. P. *Comprehensive Organometallic Chemistry*; Wilkinson, G., Stone, F. G. A., Abel, E. W., Eds.; Pergamon: Oxford, U.K., 1982; Vol. *8*, pp 1156−1159.
(17) Destabilizing interactions between the amido N lone pair and Mo filled d orbitals (a feature imposed by their saturated, 18-electron, nature) are responsible of the high instability of these species. See: Morales, D.; Pérez, J.; Riera, L.; Riera, V.; Miguel, D.; Mosquera, M. E. G.; García-Granda, S. *Chem.—Eur. J.* **2003**, *9*, 4132−4143 and references therein.
(18) Selected crystallographic data for **4b**: $C_{24}H_{25}F_3MoN_4O_5S$, M = 634.48, monoclinic, $P2_1/n$, a = 14.315(5) Å, b = 11.167(3) Å, c = 16.931(6) Å, α = 90°, β = 108.88(2)°, γ = 90°, 100.0(1) K, V = 2560(1) Å^3, Z = 4. 5532 reflections measured, 5245 independent (R_{int} = 0.0401). R1 = 0.0342, wR2 = 0.0808 (all data).
(19) The molecular structure of the cation of compound **4c** is displayed in the Supporting Information.
(20) (a) Heinze, K.; Jacob, V.; Feige, C. *Eur. J. Inorg. Chem.* **2004**, 2053−2061. (b) Curtis, M. D.; Eisenstein, O. *Organometallics* **1984**, *3*, 887−895 and references therein.
(21) For complexes **2d** and **2e** the stability of the neutral derivatives resulting from the deprotonation reaction (**3d** and **3e**, respectively) will be even lower than in the aryl derivatives **3a**−**c**, as the lone pair on the amide type nitrogen would not have the possibility of delocalization towards an aryl substituent.
(22) NOESY spectra of *tert*-buyl derivatives **2d** and **4d** showed that, as evidenced for the arylimine complexes, the η^3-allyl ligand is oriented with the open face towards the carbonyls. See the Supporting Information for further experimental details.
(23) Selected crystallographic data for **4d**: $C_{16}H_{12}F_3N_2O_8ReS$, M = 635.54, monoclinic, $P2_1/c$, a = 8.7249(1) Å, b = 15.1603(3) Å, c = 14.7401(3) Å, α = 90°, β = 91.822(2)°, γ = 90°, 100.0(1) K, V = 1948.74(6) Å^3, Z = 4. 10 569 reflections measured, 3662 independent (R_{int} = 0.0431). R1 = 0.0324, wR2 = 0.0889 (all data).
(24) Selected crystallographic data for **4e**: $C_{21}H_{27}F_3MoN_4O_5S\cdot CH_2Cl_2$, M = 685.35, triclinic, $P1$, a = 7.953(3) Å, b = 12.934(5) Å, c = 14.373(5) Å, α = 76.750(3)°, β = 87.895(3)°, γ = 76.286(3)°, 152(4) K, V = 1397(1) Å^3, Z = 2. 9654 reflections measured, 5059 independent (R_{int} = 0.0224). R1 = 0.0535, wR2 = 0.01353 (all data).
(25) (a) Leppin, J.; Föster, C.; Heinze, K. *Inorg. Chem.* **2014**, *53*, 1039−1047. (b) Jung, J.; Albright, T. A.; Hoffman, D. M.; Lee, T. R. *J. Chem. Soc., Dalton Trans.* **1999**, *24*, 4487−4494.
(26) Rikkou, M.; Manos, M.; Tolis, E.; Sigalas, M. P.; Kabanos, T. A.; Keramidas, A. D. *Inorg. Chem.* **2003**, *42*, 4640−4649.
(27) (a) Ball, G. E.; Mann, B. E. *J. Chem. Soc., Chem. Commun.* **1992**, 561−563. (b) Ascenso, J. R.; de Azevedo, C. G.; Calhorda, M. J.; Carrondo, M. A. A. F. de C. T.; Costa, P.; Dias, A. R.; Drew, M. G. B.; Félix, V.; Galvão, A. M.; Romão, C. C. *J. Organomet. Chem.* **2001**, *632*, 197−208. (c) Friend, J.; Master, S. Y.; Preece, I.; Spencer, D. M.; Taylor, K. J.; To, A.; Waters, J.; Whiteley, M. W. *J. Organomet. Chem.* **2002**, *645*, 218−227. (d) Alonso, J. C.; Neves, P.; Pires da Silva, M. J.; Quintal, S.; Vaz, P. D.; Silva, C.; Valente, A. A.; Ferreira, P.; Calhorda, M. J.; Félix, V.; Drew, M. G. B. *Organometallics* **2007**, *26*, 5548−5556.
(28) tom Dieck, H.; Friedel, J. *J. Organomet. Chem.* **1968**, *14*, 375−385.
(29) *APPEX II*; Bruker AXS Inc.: Madison, WI, 2010.
(30) Sheldrick, G. M. *SHELX-97 (SHELXS 97 and SHELXL 97), Programs for Crystal Structure Analyses*; University of Göttingen: Göttingen, Germany, 1996.
(31) *CrysAlis^{Pro} CCD, CrysAlis^{Pro} RED*; Oxford Diffraction Ltd.: Abingdon, Oxfordshire, U.K.
(32) Altomare, A.; Cascarano, G. L.; Giacovazzo, C.; Guagliardi, A.; Burla, M. C.; Polidori, G.; Camalli, M. *J. Appl. Crystallogr.* **1994**, *27*, 435−436.
(33) Sheldrick, G. M. *Acta Crystallogr.* **2008**, *A64*, 112−122.
(34) Farrugia, L. J. *J. Appl. Crystallogr.* **1997**, *30*, 565−566.
(35) Frisch, M. J.; Trucks, G. W.; Schlegel, H. B.; Scuseria, G. E.; Robb, M. A.; Cheeseman, J. R.; Scalmani, G.; Barone, V.; Mennucci, B.; Petersson, G. A.; Nakatsuji, H.; Caricato, M.; Li, X.; Hratchian, H. P.; Izmaylov, A. F.; Bloino, J.; Zheng, G.; Sonnenberg, J. L.; Hada, M.; Ehara, M.; Toyota, K.; Fukuda, R.; Hasegawa, J.; Ishida, M.; Nakajima, T.; Honda, Y.; Kitao, O.; Nakai, H.; Vreven, T.; Montgomery, J. A., Jr.; Peralta, J. E.; Ogliaro, F.; Bearpark, M.; Heyd, J. J.; Brothers, E.; Kudin, K. N.; Staroverov, V. N.; Kobayashi, R.; Normand, J.; Raghavachari, K.; Rendell, A.; Burant, J. C.; Iyengar, S. S.; Tomasi, J.; Cossi, M.; Rega, N.; Millam, J. M.; Klene, M.; Knox, J. E.; Cross, J. B.; Bakken, V.; Adamo, C.; Jaramillo, J.; Gomperts, R.; Stratmann, R. E.; Yazyev, O.; Austin, A. J.; Cammi, R.; Pomelli, C.; Ochterski, J. W.; Martin, R. L.; Morokuma, K.; Zakrzewski, V. G.; Voth, G. A.; Salvador, P.; Dannenberg, J. J.; Dapprich, S.; Daniels, A. D.; Farkas, O.; Foresman, J. B.; Ortiz, J. V.; Cioslowski, J.; Fox, D. J. *Gaussian 09, Revision A.1*; Gaussian, Inc.: Wallingford, CT, 2009.
(36) Cossi, M.; Rega, N.; Scalmani, G.; Barone, V. *J. Comput. Chem.* **2003**, *24*, 669−681.
(37) Rappé, A. K.; Casewit, C. J.; Colwell, K. S.; Goddard, W. A., III; Skiff, W. M. *J. Am. Chem. Soc.* **1992**, *114*, 10024−10039.
(38) (a) Becke, A. D. *Phys. Rev. A* **1988**, *38*, 3098−3100. (b) Lee, C.; Yang, W.; Parr, R. G. *Phys. Rev. B* **1988**, *37*, 785−789. (c) Becke, A. D. *J. Chem. Phys.* **1993**, *98*, 5648−5652.
(39) Hehre, W. J.; Radom, L.; Pople, J. A.; Schleyer, P. v. R. *Ab Initio Molecular Orbital Theory*; Wiley: New York, 1986.
(40) Hay, P. J.; Wadt, W. R. *J. Chem. Phys.* **1985**, *82*, 270−283.
(41) Ehlers, A. W.; Böhme, M.; Dapprich, S.; Gobbi, A.; Höllwarth, A.; Jonas, V.; Köhler, K. F.; Stegmann, R.; Veldkamp, A.; Frenking, G. *Chem. Phys. Lett.* **1993**, *208*, 111−114.
(42) (a) Schlegel, H. B. *J. Comput. Chem.* **1982**, *3*, 214−218. (b) Schlegel, H. B. *Theor. Chem. Acc.* **1984**, *66*, 333−340. (c) Li, X.; Frisch, M. J. *J. Chem. Theory Comput.* **2006**, *2*, 835−839.
(43) Grimme, S.; Antony, J.; Ehrlich, S.; Krieg, H. *J. Chem. Phys.* **2010**, *132*, 154104-1−154104-19.
(44) Johnson, E. R.; Becke, A. D. *J. Chem. Phys.* **2006**, *124*, 174104-1−174104-9.
(45) (a) Gonzalez, C.; Schlegel, H. B. *J. Chem. Phys.* **1989**, *90*, 2154−2161. (b) Gonzalez, C.; Schlegel, H. B. *J. Phys. Chem.* **1990**, *94*, 5523−5527.
(46) McQuarrie, D. A. *Statistical Mechanics*; Harper and Row: New York, 1976.
(47) (a) Reed, E.; Curtiss, L. A.; Weinhold, F. *Chem. Rev.* **1988**, *88*, 899−926. (b) Weinhold, F.; Carpenter, J. E. *The Structure of Small Molecules and Ions*; Naaman, R., Vager, Z., Eds.; Plenum Press: New York, 1988; pp 227−236.

DOI: 10.1021/ic502729z
Inorg. Chem. 2015, 54, 2580−2590